2464 *Inorg. Chem.* **2010**, *49*, 2464–2470
DOI: 10.1021/ic902414n

Inorganic Chemistry
Article

Theoretical Study on Activation and Protonation of Dinitrogen on Cubane-Type MIr_3S_4 Clusters (M = V, Cr, Mn, Fe, Co, Ni, Cu, Mo, Ru, and W)

Hiromasa Tanaka,[†] Fumihiro Ohsako,[†] Hidetake Seino,[‡] Yasushi Mizobe,[‡] and Kazunari Yoshizawa*[,†]

[†]*Institute for Materials Chemistry and Engineering, Kyushu University, Fukuoka 819-0395, Japan, and*
[‡]*Institute of Industrial Science, The University of Tokyo, Tokyo 153-8505, Japan*

Received December 4, 2009

Density functional theory (DFT) calculations on cubane-type metal−sulfido clusters MIr_3S_4 ligating N_2 (M = V, Cr, Mn, Fe, Co, Ni, Cu, Mo, Ru, and W) have been performed for the proposal of new clusters that can highly activate N_2 beyond the $RuIr_3S_4$ cluster prepared by Mizobe and co-workers [*Angew. Chem. Int. Ed.* **2007**, *46*, 5431]. The degree of N_2 activation in the metal−N_2 complexes was evaluated based on the N−N bond distance and vibrational frequency and the gross atomic charge on N_2. The degree of N_2 activation strongly depends on the metal atoms at the N_2-binding site, and the $MoIr_3S_4$ and WIr_3S_4 clusters exhibit significant N_2-activation ability. The reactivity of the MIr_3S_4−N_2 complexes (M = Ru, Mo, and W) with a proton donor (lutidinium) has been discussed from a kinetic aspect by exploring a possible reaction pathway of proton transfer. The protonation of the Ru−N_2 complex would not occur due to a very high-activation barrier and to an instability of the Ru−NNH^+ complex, which is consistent with our present experimental result that the Ru−N_2 complex has not been protonated at room temperature. On the other hand, the protonation of the Mo−N_2 and W−N_2 complexes would proceed smoothly from DFT criteria. The result of calculations indicates that the Mo and W clusters are best suited for the protonation of N_2, which is the first step toward nitrogen fixation.

1. Introduction

Nitrogen fixation, which is the reduction of atmospheric dinitrogen to ammonia, is one of the most important and fascinating catalytic reactions in biology and chemistry.[1] Dinitrogen is chemically inert due to the nonpolar and extremely strong triple bond (225 kcal/mol) and the large highest occupied molecular orbital−lowest unoccupied molecular orbital (HOMO−LUMO) gap. Both artificial and biological nitrogen fixations are mediated by metal-based catalysts. Artificial nitrogen fixation, typified by the Haber-Bosch process, converts dinitrogen and dihydrogen into ammonia on the surface of an iron catalyst under drastic reaction conditions of high pressure and high temperature. In contrast, biological nitrogen fixation is attained by enzyme nitrogenases in certain bacteria under ambient conditions.[2] Among the three types of nitrogenases, i.e., Mo−Fe, V−Fe, and Fe−Fe nitrogenases, the most well-studied MoFe nitrogenase contains a corner-shared, double cubane-type Fe−Mo−S cluster $MoFe_7S_9X$ called the FeMo cofactor at its active site, where X is an unknown element (probably N, C, or O).[3] Dinitrogen bound to the FeMo cofactor is reduced to ammonia according to the optimal reaction (eq 1), in which 8 proton/electron pairs and 16 MgATPs are consumed for the formation of $2NH_3$ and for the mandatory evolution of H_2.

$$N_2 + 8H^+ + 8e^- + 16MgATP \rightarrow 2NH_3 + H_2 + 16MgADP + 16P_i \quad (1)$$

In the process of nitrogen fixation, the first hydrogenation of dinitrogen yielding an diazenido (−NNH) intermediate is known to be energetically the most difficult step.[4] Although a great deal of effort has been devoted to experimental[5] and

*Corresponding author. E-mail: kazunari@ms.ifoc.kyushu-u.ac.jp.

(1) (a) MacKey, B. A.; Fryzuk, M. D. *Chem. Rev.* **2004**, *104*, 385–401. (b) Shaver, M. P.; Fryzuk, M. D. *Adv. Synth. Catal.* **2003**, *345*, 1061. (c) Himmel, H.-J.; Reiher, M. *Angew. Chem., Int. Ed. Engl.* **2006**, *45*, 6264. (d) Rees, D. C.; Howard, J. B. *Curr. Opin. Chem. Biol.* **2000**, *4*, 559. (e) Fisher, K.; Newton, W. E. *Nitrogen Fixation at the Millenium*; Leigh, G. J., Ed.; Elsevier Science B. V.: Amsterdam, The Netherlands, 2002; pp 1−34.

(2) (a) Rees, D.; Tezcan, F. A.; Haynes, C. A.; Walton, M. Y.; Andrade, S.; Einsle, O.; Howard, J. B. *Phil. Trans. R. Soc. A* **2005**, *363*, 971. (b) Igarashi, R. Y.; Seefeldt, L. C. *Crit. Rev. Biochem. Mol. Biol.* **2003**, *38*, 351. (c) Burgess, B. K.; Lowe, D. J. *Chem. Rev.* **1996**, *96*, 2983. (d) Eady, R. R. *Chem. Rev.* **1996**, *96*, 3013. (e) Howard, J. B.; Rees, D. C. *Chem. Rev.* **1996**, *96*, 2965.

(3) Einsle, O.; Tezcan, F. A.; Andrade, S. L. A.; Schmid, B.; Yoshida, M.; Howard, J. B.; Rees, D. C. *Science* **2002**, *297*, 1696.

(4) Durrant, M. C. *Biochem.* **2002**, *41*, 13934.

(5) (a) Dos Santos, P. C.; Dean, D. R.; Hu, Y.; Ribbe, M. W. *Chem. Rev.* **2004**, *104*, 1159. (b) Seefeldt, L. C.; Dance, I. G.; Dean, D. R. *Biochem.* **2004**, *43*, 1401. (c) Barney, B. M.; Laryukhin, M.; Igarashi, R. Y.; Lee, H.-I.; Dos Santos, P. C.; Yang, T.-C.; Hoffman, B. M.; Dean, D. R.; Seefeldt, L. C. *Biochem.* **2005**, *44*, 8030. (d) Barney, B. M.; Yang, T.-C.; Igarashi, R. Y.; Dos Santos, P. C.; Laryukhin, M.; Lee, H.-I.; Hoffman, B. M.; Dean, D. R.; Seefeldt, L. C. *J. Am. Chem. Soc.* **2005**, *127*, 14960. (e) Barney, B. M.; McClead, J.; Lukoyanov, D.; Laryukhin, M.; Yang, T.-C.; Dean, D. R.; Hoffman, B. M.; Seefeldt, L. C. *Biochem.* **2007**, *46*, 6784.

Published on Web 02/02/2010

theoretical[6] research on elucidating the biological nitrogen fixation process mediated by nitrogenases, the questions on where dinitrogen is bound in the FeMo cofactor and how dinitrogen is reduced to ammonia are still unanswered.

Cubane-type metal−sulfido clusters have been receiving much attention as structural and functional models of the active site of nitrogenases.[7] These clusters have a cuboidal core whose corners are alternatively occupied by four metal atoms and by four sulfido ligands bridging the metals. The chemistry of the well-defined metal−sulfido clusters ligating dinitrogen or its related nitrogenous substrates will provide a valuable insight into the elucidation of coordination mode and reactivity of substrate molecules bound to the active site of nitrogenases. Coucouvanis and co-workers[8] prepared cubane-type MFe_3S_4 (M = Mo and V) clusters that can catalytically reduce hydrazine (N_2H_4) into ammonia, while Hidai, Mizobe, and co-workers[9] demonstrated the catalytic N−N bond cleavage of hydrazine with cubane-type $RuMo_3S_4$ and $Mo_2M_2S_4$ (M = Ir and Rh) clusters. However, no cubane-type metal−sulfido clusters were known that can bind or reduce N_2 in a well-defined manner;[10] although Tanaka et al.[11] reported the formation of some ammonia by means of the electro-reduction of N_2 in the presence of $MoFe_3S_4$ clusters. This shows a clear contrast to the fact that a great number of well-defined N_2 complexes have been isolated for almost all d-block transition metals as well as some f-block metals supported by various ancillary ligands, such as phosphines, cyclopentadienyls, amides, and less commonly thiolates.[1a,b,12] It also seems strange that metal−N_2 complexes supported by sulfur-based ancillary ligands are uncommon,[13] although metal atoms are bridged by sulfur atoms in the FeMo cofactor.

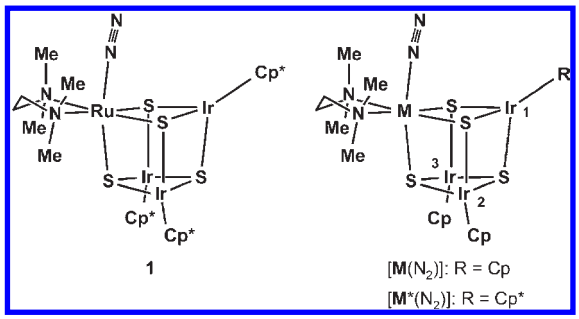

Figure 1. The $RuIr_3S_4$−N_2 complex $[(Cp^*Ir)_3\{Ru(tmeda)(N_2)\}(\mu_3\text{-}S)_4]$ (**1**) and model complexes [**M**(N_2)] and [**M***(N_2)] (**M** = V, Cr, Mn, Fe, Co, Ni, Cu, Mo, Ru, and W).

Recently Mizobe and co-workers[14] have succeeded in the isolation of a cubane-type metal−sulfido cluster having dinitrogen as a ligand: $[(Cp^*Ir)_3\{Ru(tmeda)(N_2)\}(\mu_3\text{-}S)_4]$ (**1**; $Cp^* = \eta^5\text{-}C_5Me_5$) shown in Figure 1. According to an X-ray crystallographic analysis, the N_2 ligand in **1** coordinates at the Ru atom in an end-on manner. The N−N stretching of 2 019 cm^{-1}, which is considerably red-shifted relative to that of a free dinitrogen (2 331 cm^{-1}), indicates that the triple bond of N_2 is effectively weakened upon coordination to the $RuIr_3S_4$ cluster. In the previous study, we discussed the feasibility of the $RuIr_3S_4$ cluster as a catalyst for nitrogen fixation by density functional theory (DFT) calculations.[15] The calculational result showed that the N≡N bond of the N_2 ligand is reductively activated by complexation and that the Ru−N_2 binding energy (16.4 kcal/mol) is large enough to form a metal−N_2 complex. The reduction of N_2 catalyzed by a simplified model of **1**, $[(CpIr)_3\{Ru(tmeda)\}(\mu_3\text{-}S)_4]$ ([**Ru**]; $Cp = \eta^5\text{-}C_5H_5$), was examined based on the Yandulov−Schrock cycle, proposed as a mechanism of nitrogen fixation mediated by a Mo−triamidoamine complex [Mo(hiptN_3N)] (hiptN_3N = hexaisopropyl-terphenyl-triamidoamine).[16] This Mo complex is the first example that succeeded in the catalytic conversion of N_2 into NH_3 using a combination of proton and electron donors, lutidinium ($LutH^+$; Lut = 2,6-dimethylpyridine), and decamethylchromocene (Cp^*_2Cr). The Yandulov−Schrock cycle assumes successive hydrogenations of the end-on coordinated N_2 through alternating steps of protonation and reduction, and its validity is strongly supported by the isolation and observation of a large part of intermediates as well as intensive theoretical studies on the catalytic cycle.[17] This mechanism was applied for the $RuIr_3S_4$

(6) (a) Dance, I. *Chem. Asian J.* **2007**, *2*, 936. (b) Kästner, J.; Blöchl, P. *J. Am. Chem. Soc.* **2007**, *129*, 2998. (c) Dance, I. *Biochem.* **2006**, *45*, 6328. (d) Dance, I. *J. Am. Chem. Soc.* **2005**, *127*, 10925. (e) Huniar, U.; Ahlrichs, R.; Coucouvanis, D. *J. Am. Chem. Soc.* **2004**, *126*, 2588. (f) Schimpl, J.; Petrilli, H. M.; Blöchl, P. E. *J. Am. Chem. Soc.* **2003**, *125*, 15772. (g) Lovell, T.; Liu, T.; Case, D. A.; Noodleman, L. *J. Am. Chem. Soc.* **2003**, *125*, 8377. (h) Durrant, M. C. *Biochem.* **2002**, *41*, 13946. (i) Hinnermann, B.; Nørskov, J. K. *J. Am. Chem. Soc.* **2003**, *125*, 1466. (j) Siegbahn, P. E. M.; Westerberg, J.; Svensson, M.; Crabtree, R. J. *J. Phys. Chem. B* **1998**, *102*, 1615. (k) Deng, H. B.; Hoffmann, R. *Angew. Chem., Int. Ed.* **1992**, *32*, 1062.

(7) (a) Hidai, M.; Mizobe, Y. *Can. J. Chem.* **2005**, *83*, 358. (b) Hidai, M.; Kuwata, S.; Mizobe, Y. *Acc. Chem. Res.* **2000**, *33*, 46. (c) Henderson, R. A. *Chem. Rev.* **2005**, *105*, 2365. (d) Ohki, Y.; Ikagawa, Y.; Tatsumi, K. *J. Am. Chem. Soc.* **2007**, *129*, 10457. (e) Lee, S. C.; Holm, R. H. *Chem. Rev.* **2004**, *104*, 1135. (f) Ohki, Y.; Sunada, Y.; Honda, M.; Katada, M.; Tatsumi, K. *J. Am. Chem. Soc.* **2003**, *125*, 4052.

(8) (a) Coucouvanis, D.; Demadis, K. D.; Malinak, S. M.; Mosier, P. E.; Tyson, M. A.; Laughlin, L. J. *J. Mol. Catal. A: Chem.* **1996**, *107*, 123. (b) Demadis, K. D.; Malinak, S. M.; Coucouvanis, D. *Inorg. Chem.* **1996**, *35*, 4038. (c) Malinak, S. M.; Demadis, K. D.; Coucouvanis, D. *J. Am. Chem. Soc.* **1995**, *117*, 3126.

(9) (a) Takei, I.; Dohki, K.; Kobayashi, K.; Suzuki, T.; Hidai, M. *Inorg. Chem.* **2005**, *44*, 3768. (b) Seino, H.; Masumori, T.; Hidai, M.; Mizobe, Y. *Organometallics* **2003**, *22*, 3424.

(10) (a) Kozlowski, P. M.; Shiota, Y.; Gomita, S.; Seino, H.; Mizobe, Y.; Yoshizawa, K. *Bull. Chem. Soc. Jpn.* **2007**, *80*, 2323. (b) Takei, I.; Kobayashi, K.; Dohki, K.; Nagao, S.; Mizobe, Y.; Hidai, M. *Chem. Lett.* **2007**, *36*, 546. (c) Yoshizawa, K.; Kihara, N.; Shiota, Y.; Seino, H.; Mizobe, Y. *Bull. Chem. Soc. Jpn.* **2006**, *79*, 53.

(11) Tanaka, K.; Hozumi, Y.; Tanaka, T. *Chem. Lett.* **1982**, 1203.

(12) (a) Hidai, M.; Mizobe, Y. *Chem. Rev.* **1995**, *95*, 1115. (b) Chatt, J; Dilworth, J. R.; Richards, R. L. *Chem. Rev.* **1978**, *78*, 589. (c) Allen, A. D.; Harris, R. O.; Loescher, B. R.; Stevens, J. R.; Whiteley, R. N. *Chem. Rev.* **1973**, *73*, 11.

(13) (a) Sellmann, D.; Hautsch, B.; Rösler, A.; Heinemann, F. W. *Angew. Chem., Int. Ed. Engl.* **2001**, *40*, 1505. (b) Sellmann, D.; Hille, A.; Heinemann, F. W.; Moll, M.; Rösler, A.; Sutter, J.; Brehm, G.; Reiher, M.; Hess, B. A.; Schneider, S. *Inorg. Chim. Acta* **2003**, *348*, 194. (c) Sellmann, D.; Hille, A.; Rösler, A.; Heinemann, F. W.; Moll, M.; Brehm, G.; Schneider, S.; Reiher, M.; Hess, B. A.; Bauer, W. *Chem.—Eur. J.* **2004**, *10*, 819. (d) Reiher, M.; Salomon, O.; Sellmann, D.; Hess, B. A. *Chem.—Eur. J.* **2001**, *7*, 5195. (e) Reiher, M.; Kirchner, B.; Hutter, J.; Sellmann, D.; Hess, B. A. *Chem.—Eur. J.* **2004**, *10*, 4443. (f) Kirchner, B.; Reiher, M.; Hille, A.; Hutter, J.; Hess, B. A. *Chem.—Eur. J.* **2005**, *11*, 574.

(14) Mori, H.; Seino, H.; Hidai, M.; Mizobe, Y. *Angew. Chem., Int. Ed. Engl.* **2007**, *46*, 5431.

(15) Tanaka, H.; Mori, H.; Seino, H.; Hidai, M.; Mizobe, Y.; Yoshizawa, K. *J. Am. Chem. Soc.* **2008**, *130*, 9037.

(16) (a) Yandulov, D. V.; Schrock, R. R. *Science* **2003**, *301*, 76. (b) Schrock, R. R. *Acc. Chem. Res.* **2005**, *38*, 955.

(17) (a) Schrock, R. R. *Angew. Chem., Int. Ed. Engl.* **2008**, *47*, 2. (b) Schenk, S.; Le Guennic, B.; Kirchner, B.; Reiher, M. *Inorg. Chem.* **2008**, *47*, 3634. (c) Magistrato, A.; Robertazzi, A.; Carloni, P. *J. Chem. Theory Comput.* **2007**, *3*, 1708. (d) Hölscher, M.; Leitner, W. *Eur. J. Inorg. Chem.* **2006**, 4407. (e) Reiher, M.; Le Guennic, B.; Kirchner, B. *Inorg. Chem.* **2005**, *44*, 9640. (f) Le Guennic, B.; Kirchner, B.; Reiher, M. *Chem.—Eur. J.* **2005**, *11*, 7448. (g) Studt, F.; Tuczek, F. *Angew. Chem., Int. Ed. Engl.* **2005**, *44*, 5639. (h) Cao, Z.; Zhou, Z.; Wan, H.; Zhang, Q. *Int. J. Quantum Chem.* **2005**, *103*, 344.

cluster system with $LutH^+$ and decamethylcobaltocene (Cp^*_2Co) as a pair of proton/electron donors.[15] As a result, we demonstrated that the reduction of N_2 on the $RuIr_3S_4$ cluster proceeds in an exothermic way, except for the first protonation of N_2 and the release of the second molecule of NH_3. The calculated energy profile for the $RuIr_3S_4$ cluster has indicated that this cluster is capable of serving as a catalyst for nitrogen fixation if an appropriate pair of proton/electron donors is chosen. Another finding to be noted here is that a diazenido intermediate has a unique *cis*-bent Ru−N−N−H linkage, which is ascribed to a cooperative binding of a hydrogen atom by the N_2 ligand and an iridium atom in the cubane framework. The stabilization of the diazenido intermediate by the cooperative binding would reduce the disadvantage in the enthalpy change for the first protonation of N_2.

Contrary to the promising result of calculations, there has been no experimental evidence for the formation of ammonia from the $RuIr_3S_4$ cluster by protonation alone or by coupled protonation/electronation up to now. We have observed only the liberation of N_2 gas followed by catalytic evolution of H_2 gas. This result suggests that the $RuIr_3S_4$ cluster can activate the coordinated N_2 significantly, but the degree of activation is not sufficient for the functionalization of N_2. However, we still believe that the cuboidal core, comprised of one transition-metal atom, three iridium atoms, and four sulfur atoms, is a good candidate as the site for aiming at effective reduction of N_2 because, at present, the $RuIr_3S_4$ cluster is the only example of the cubane-type metal−sulfido complexe that can bind N_2 and the N_2 ligand is activated more highly than those of any other precedent Ru(II) and Ru(0) complexes, at least from the criteria of the N−N stretching. Replacing Ru at the binding site of N_2 by another transition metal may drastically change the N_2-activating ability. It is known that the reactivity of coordinated N_2 depends on various factors, such as the metal at the binding site, the ancillary ligands, and the acid (reductant).[18] Indeed, in the case of Schrock's Mo−triamidoamine complex, the [M(hiptN$_3$N)] complexes (M = V, Cr, and W) do not exhibit catalytic activity for N_2 reduction.[19]

In the present study, we have figured out the degree of N_2 activation in the MIr_3S_4 complexes ligating N_2 (M = V, Cr, Mn, Fe, Co, Ni, Cu, Mo, and W) by DFT calculations to propose a new cubane-type metal−sulfido cluster that has high N_2-activating ability beyond the $RuIr_3S_4$ cluster. The degree of N_2 activation in a metal−N_2 complex is experimentally judged from elongation of the N−N bond and the red-shift of the N−N stretching frequency relative to free N_2. Atomic charges on N_2, which are computationally available, are also a useful criterion for judging the degree of N_2 activation. Dinitrogen must be attacked by H^+ at the first step toward biomimetic nitrogen fixation, and therefore, the reactivity of coordinated N_2 with H^+ should closely correlate with the amount of negative charge assigned to the N_2 moiety. For some mononuclear Mo and W complexes having an end-on coordinated N_2, Deeth and Field[20] as well as Studt and Tuczek[21] pointed out a correlation between the gross charges on N_2 and the experimental results on the reactivity of N_2 with proton. For quantitative predictions of the reactivity of the MIr_3S_4−N_2 complexes, the first protonation of N_2 coordinated to the MIr_3S_4 clusters has also been investigated theoretically. It is to be noted that this process is quite important for initiation of N_2 reduction but is known to be the most difficult step in the cycle converting N_2 into ammonia.

2. Computational Method

All calculations were carried out with the Jaguar 7.0 program package.[22] Calculated model complexes shown in Figure 1 were constructed based on the X-ray crystal structure of $[(Cp^*Ir)_3\{Ru(tmeda)(N_2)\}(\mu_3\text{-}S)_4]$ **1**, and the ruthenium atom at the N_2 binding site was replaced by another transition metal (V, Cr, Mn, Fe, Co, Ni, Cu, Mo, and W). The three Cp* ligands in **1** were replaced by the Cp (η^5-C_5H_5) ligands in [**M**(N_2)] (Figure 1). The simplification of the Cp* ligands in **1** would not change the geometry in the vicinity of the N_2 ligand.[15] Protonated species having the N_2H^+ ligand, $[\mathbf{M}(N_2H)]^+$, were optimized for the Ru, Mo, and W cores. For these cores, substitution effects of the ligand R on Ir1 (see Figure 1) were discussed by comparing optimized structures of the Cp- and Cp*-substituted complexes. The bulkiness of the ligand R should be considered particularly for the protonated complexes because Ir1 in $[\mathbf{Ru}(N_2H)]^+$ supports the protonation of N_2 through the bonding interaction between Ir1 and H^+.[15] The Cp*-substituted complexes are distinguished from the Cp-substituted ones by an asterisk after **M** ([**M***(N_2)] and $[\mathbf{M}^*(N_2H)]^+$). The reactivity of [**M**(N_2)] (**M** = Ru, Mo, or W) with a proton was assessed by exploring the reaction pathway of the proton transfer from $LutH^+$ to the N_2 ligand in [**M**(N_2)]. To discuss the energetics of the proton transfer process, we optimized a reactant complex (**RC**), a product complex (**PC**), and the transition state (**TS**) connecting them. Solvent effects were taken into account with a self-consistent reaction field method using the Poisson−Boltzmann solver[23], and tetrahydrofuran (THF; ε = 7.58) was chosen as the solvent.

Optimizations and vibrational analyses were performed at the B3LYP/LACVP+* level of theory.[24,25] Total energies of the **RC**, **PC**, and **TS** were obtained with single-point calculations at their optimized structures using a larger basis set LACV3P+**. LACVP+* represents a mixed basis set using the LanL2DZ relativistic effective core potential (RECP) for metal atoms and the 6-31+G(d) basis set for all other atoms. In the LACV3P+** basis set, the 6-311+G(d,p) basis set is used instead of the 6-31+G(d) basis set. Vibrational frequencies were corrected by a scale factor of 0.96.[26] Atomic charges

(18) (a) Spencer, L. P.; MacKay, B. A.; Patrick, B. O.; Fryzuk, M. D. *Proc. Natl. Acad. Sci. U.S.A.* **2006**, *103*, 17094. (b) Leigh, G. J. *Acc. Chem. Res.* **1992**, *25*, 177.

(19) (a) Smythe, N. C.; Schrock, R. R.; Müller, P.; Weare, W. W. *Inorg. Chem.* **2006**, *45*, 7111. (b) Yandulov, D. V.; Schrock, R. R. *Can. J. Chem.* **2005**, *83*, 341. (c) Smythe, N. C.; Schrock, R. R.; Müller, P.; Weare, W. W. *Inorg. Chem.* **2006**, *45*, 9197.

(20) Deeth, R. J.; Field, C. N. *J. Chem. Soc., Dalton Trans.* **1994**, 1943.

(21) (a) Studt, F.; Tuczek, F. *J. Comput. Chem.* **2006**, *27*, 1278. (b) Habeck, C. M.; Lehnert, N.; Näther, C.; Tuczek, F. *Inorg. Chim. Acta* **2002**, *337*, 11.

(22) *Jaguar*, version 7.0; Schrödinger, LLC: New York, NY, **2007**.

(23) (a) Tannor, D. J.; Marten, B.; Murphy, R.; Friesner, R. A.; Sitkoff, D.; Nicholls, A.; Ringnalda, M.; Goddard, W. A., III; Honig, B. *J. Am. Chem. Soc.* **1994**, *116*, 11875. (b) Marten, B.; Kim, K.; Cortis, C.; Friesner, R. A.; Murphy, R. B.; Ringnalda, M. N.; Sitkoff, D.; Honig, B. *J. Phys. Chem.* **1996**, *100*, 11775.

(24) (a) Becke, A. D. *Phys. Rev. A: At., Mol., Opt. Phys.* **1988**, *38*, 3098. (b) Becke, A. D. *J. Chem. Phys.* **1993**, *98*, 5648. (c) Lee, C.; Yang, W.; Parr, R. G. *Phys. Rev. B: Condens. Matter* **1988**, *37*, 785. (d) Stephens, P. J.; Devlin, F. J.; Chabalowski, C. F.; Frisch, M. J. *J. Phys. Chem.* **1994**, *98*, 11623.

(25) (a) Ditchfield, R.; Hehre, W. J.; Pople, J. *A. J. Chem. Phys.* **1971**, *54*, 724. (b) Hehre, W. J.; Ditchfield, R.; Pople, J. A. *J. Chem. Phys.* **1972**, *56*, 2257. (c) Hariharan, P. C.; Pople, J. A. *Theor. Chim. Acta* **1973**, *28*, 213. (d) Clark, T.; Chandrasekhar, J.; Spitznagel, G. W.; Schleyer, P. v. R. *J. Comput. Chem.* **1983**, *4*, 294. (e) Francl, M. M.; Petro, W. J.; Hehre, W. J.; Binkley, J. S.; Gordon, M. S.; DeFrees, D. J.; Pople, J. A. *J. Chem. Phys.* **1982**, *77*, 3654. (f) Hay, P. J.; Wadt, W. R. *J. Chem. Phys.* **1985**, *82*, 299.

(26) Scott, A. P.; Radom, L. *J. Phys. Chem.* **1996**, *100*, 16502.

Table 1. Characteristics of N_2 Coordinated to MIr_3S_4 Clusters (M = V, Cr, Mn, Fe, Co, Mo, Ru, and W) Calculated at the B3LYP/LACVP+* Level of Theory[a]

M	V	Cr	Mn	Fe	Co	Mo	Ru[b]	W	free N_2[c]
S [**M**(N_2)]	1.5	1.0	1.5	0.0	0.5	0.0	0.0	0.0	
S [**M**]	1.5	2.0	2.5	2.0	1.5	2.0	0.0	1.0	
r_{NN}	1.118	1.135	1.124	1.121	1.114	1.150	1.128	1.161	1.0977
ν_{NN}	2161	2045	2075	2170	2234	1952	2118	1889	2358.6
q_{NN}	−0.03	−0.18	−0.15	−0.06	−0.09	−0.33	−0.10	−0.49	
BDE	5.4	16.1	3.7[d]	12.5	< 0.5[d]	22.0	19.2	20.0	

[a] S represents the spin quantum number of the ground state, r_{NN} is the N−N distance in Å, ν_{NN} is the N−N stretching frequency in cm^{-1}, q_{NN} is the gross NPA charge on N_2, and BDE is the bond dissociation energy between the MIr_3S_4 core and the N_2 in kcal/mol. [b] Ref 15. [c] Ref 28. [d] See Supporting Information.

were calculated with the natural population analysis (NPA).[27] For [**Ru**(N_2)] we confirmed that the LACVP+* basis set with the double-ζ quality gives geometric parameters and vibrational frequencies comparable to that of the LACV3P+** basis set with the triple-ζ quality. The total charge of [**M**(N_2)] and [**M**(N_2H)]$^+$ is zero and +1, respectively. Since the formal charge of the Cp ring is −1 and the sulfur atom is −2, the M and Ir atoms in [**M**(N_2)] are supposed to have the formal charges of +2 and +3, respectively.

3. Results and Discussion

3.1. Dinitrogen Complexes $MIr_3S_4-N_2$. Calculated characteristics of the N_2 ligand in [**M**(N_2)] (**M** = V, Cr, Mn, Fe, Co, Mo, Ru, and W) are listed in Table 1. Dinitrogen-coordinated Ni and Cu complexes were not successfully optimized for any spin states. For Mn and Co, although optimized structures of [**Mn**(N_2)] and [**Co**(N_2)] were found to be local minima with no imaginary frequencies, the calculated total energies lie above the dissociation limit of [**M**] and N_2 (see Supporting Information). We first discuss how the degree of N_2 activation depends on the metal atom **M** on the basis of four parameters: (i) the N−N bond distance, (ii) N−N stretching frequency (ν_{NN}), (iii) gross NPA charge on N_2 (q_{NN}), and (iv) bond dissociation energy (BDE) between [**M**] and N_2. The BDEs are calculated based on the reaction [**M**] + N_2 → [**M**(N_2)], where [**M**] and [**M**(N_2)] have the ground-state structure and may have different spin states. For example, the ground-state structures of [**Mo**] and [**Mo**(N_2)] have the spin quintet and singlet, respectively.

A striking finding is that the MIr_3S_4 core containing a d^4 metal, particularly Mo and W, exhibits a high N_2-activating ability. The N−N distance and the ν_{NN} of [**Mo**(N_2)] ([**W**(N_2)]) are calculated to be 1.150 (1.161) Å and 1952 (1889) cm^{-1}, respectively, both the cores having a N_2-activating ability superior to that of the Ru core experimentally prepared.[14] The gross NPA charges on N_2 (−0.33 for Mo and −0.49 for W) suggest that the coordinated N_2 is significantly reduced by the Mo and W core. The M−N_2 bond energies of [**Mo**(N_2)] and [**W**(N_2)] are 22.0 and 20.0 kcal/mol, respectively, which are comparable to that of the prepared [**Ru**(N_2)] (19.2 kcal/mol). Thus, the Mo−N_2 and W−N_2 complexes are considered to be isolable if the $MoIr_3S_4$ and WIr_3S_4 cores are synthesized. The VIr_3S_4 and $FeIr_3S_4$ cores exhibit poor N_2-activating ability relative to those of the d^4-metal and Ru cores. Kozlowski et al.[10a] reported that [(Cp*Ir)$_3$(FeCl)(μ-S)$_4$] having a cuboidal $FeIr_3S_4$ core did not bind dinitrogen.

Table 2. Characteristics of N_2 Coordinated to [**M***] (M = Mo, Ru, and W) Calculated at the B3LYP/LACVP+* Level of Theory[a]

	Mo	Ru	W
S [**M***(N_2)]	0.0	0.0	0.0
S [**M***]	2.0	0.0	1.0
r_{NN}	1.153	1.129	1.164
ν_{NN}	1933	2109	1870
q_{NN}	−0.35	−0.11	−0.51
BDE	23.2	19.5	22.3

[a] S represents the spin quantum number of the ground state, r_{NN} is the N−N distance in Å, ν_{NN} is the N−N stretching frequency in cm^{-1}, q_{NN} is the gross NPA charge on N_2, and BDE is the bond dissociation energy in kcal/mol between the Cp*-substituted MIr_3S_4 cluster core and N_2.

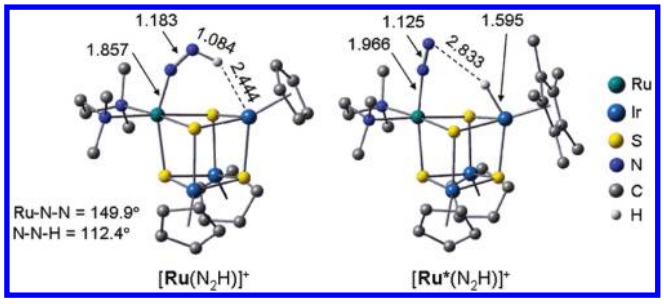

Figure 2. Optimized structures of [**Ru**(N_2H)]$^+$ and [**Ru***(N_2H)]$^+$. Hydrogen atoms except for the added proton are omitted for clarity. Interatomic distances are presented in Å.

Characteristics of the N_2 ligand in [**M***(N_2)] (M = Ru, Mo, and W) are summarized in Table 2. Replacing the Cp ligand on Ir1 by the Cp* ligand influences neither the characteristics of the N_2 ligand nor the strength of the M−N_2 bond.

3.2. Protonated Complexes $MIr_3S_4-N_2H^+$ (M = Ru, Mo, and W). Contrary to $MIr_3S_4-N_2$ complexes, optimized structures of the protonated complexes are very sensitive to both the bulkiness of the ligand R and the metal atom at the coordination site of N_2. Figures 2 and 3 show the optimized structures of [**M**(N_2H)]$^+$ and [**M***(N_2H)]$^+$ for **M** = Ru, Mo, and W. While the optimized structure of [**Ru**(N_2H)]$^+$ has a diazenido (−NNH) group with a strongly *cis*-bent Ru−N−N−H linkage (Ru−N−N = 149.9°), [**Ru***(N_2H)]$^+$ adopts a structure in which the added H^+ is attracted to Ir1 to form an Ir−H bond (Ir−H = 1.595 Å). The separated coordination of N_2 and H in [**Ru***(N_2H)]$^+$ would stem from the narrow space surrounded by the bulkier Cp* ligand and the Ru(μ-S)$_2$Ir plane (Figure 4). The N_2−H

(27) Glendening, E. D.; Badenhoop, J. K.; Reed, A. E.; Carpenter, J. E.; Bohmann, J. A.; Morales, C. M.; Weinhold, F. *NBO 5.0*; Theoretical Chemistry Institute, University of Wisconsin: Madison, WI, **2001**; http://www.chem.wisc.edu/~nbo5

(28) (a) Huber, K. P.; Herzberg, G. *Molecular Spectra and Molecular Structure. IV. Constants of Diatomic Molecules*; Van Nostrand Reinhold Co.: New York, 1979. (b) Shimanouchi, T. *National Bureau of Standards Reference Data Series*; National Bureau of Standards: Garthersburg, MD, 1972; Vol. *I*.

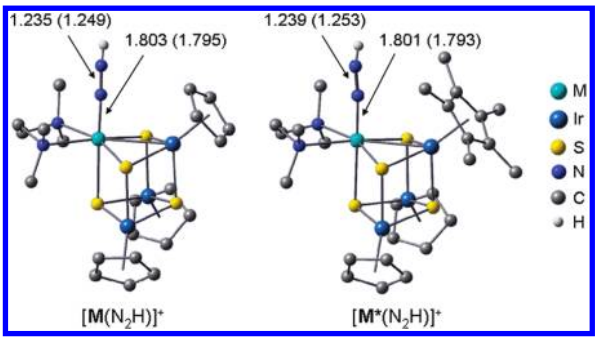

Figure 3. Optimized structures of $[\mathbf{M}(N_2H)]^+$ and $[\mathbf{M}^*(N_2H)]^+$ (**M** = Mo and W). Hydrogen atoms except for the added proton are omitted for clarity. Bond distances (in Å) for M = W are shown in parentheses. Selected bond distances and angles for $[\mathbf{M}(N_2H)]^+$: **M**−Ir1 = 2.918 (2.925), N−H = 1.032 (1.031), **M**−N−N = 173.2° (173.4°), and N−N−H = 113.3° (112.1°). Selected bond distances and angles for $[\mathbf{M}^*(N_2H)]^+$: **M**−Ir1 = 2.927 (2.941), N−H = 1.032 (1.031), **M**−N−N = 171.7° (172.3°), and N−N−H = 112.8° (111.8°).

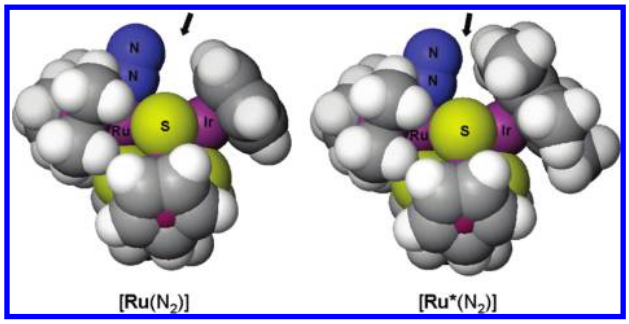

Figure 4. Space-filling models of the optimized structures of $[\mathbf{Ru}(N_2)]$ and $[\mathbf{Ru}^*(N_2)]$.

bond in $[\mathbf{Ru}(N_2H)]^+$ is supported by Ir1 through a bonding interaction between Ir and H. In $[\mathbf{Ru}^*(N_2H)]^+$, however, the bulkier Cp* ligand on Ir1 prevents a proton from occupying an appropriate position between the N_2 ligand and the Ir1. The calculational result on $[\mathbf{Ru}^*(N_2H)]^+$ implies that the N_2 ligand in the experimentally prepared **1** cannot be protonated.

As shown in Figure 3, the N_2 ligand in $[\mathbf{Mo}(N_2)]$ and $[\mathbf{W}(N_2)]$ can be protonated to yield diazenido complexes having a nearly linear M−N−N linkage. The optimized M−N−N bond angles in $[\mathbf{M}(N_2H)]^+$ are 173.2° for Mo and 173.4° for W, which are commonly observed in metal−diazenido complexes.[12a,29] The bulkiness of the ligand R does not influence the geometry in the vicinity of N_2H on the Mo and W cores. The N−H, N−N, and Mo−N distances in $[\mathbf{Mo}(N_2H)]^+$ ($[\mathbf{W}(N_2H)]^+$) are calculated to be 1.032 (1.031), 1.235 (1.249), and 1.803 (1.794) Å, while those values in $[\mathbf{Mo}^*(N_2H)]^+$ ($[\mathbf{W}^*(N_2H)]^+$) are 1.032 (1.031), 1,239 (1.253), and 1.801 (1.793) Å, respectively. These optimized structures indicate that the N_2 ligand coordinated to the Mo and W cores is capable of binding proton without any supports.

3.2. Protonation of N_2 Ligand in $[\mathbf{M}(N_2)]$ and $[\mathbf{M}^*(N_2)]$. We previously discussed the protonation of $[\mathbf{Ru}(N_2)]$ with $LutH^+$ from a thermodynamical aspect based on a thermochemical equation $[\mathbf{Ru}(N_2)] + LutH^+ \rightarrow [\mathbf{Ru}(N_2H)]^+ + Lut$.[15] The enthalpy change in the protonation is calculated by treating $[\mathbf{Ru}(N_2)]$ and $LutH^+$ separately at an infinite distance. A calculated enthalpy change (ΔH_0 = +17.8 kcal/mol) showed that the N_2 ligand in $[\mathbf{Ru}(N_2)]$ can be protonated with $LutH^+$. However, structural differences between $[\mathbf{Ru}(N_2H)]^+$ and $[\mathbf{Ru}^*(N_2H)]^+$ urge us to examine how the bulkiness of the ligand R on Ir1 influences the process of protonation. We here assess the reactivity of the $MIr_3S_4-N_2$ (M = Ru, Mo, and W) complexes with $LutH^+$ from a kinetic aspect of proton transfer. The activation energy (E_a) for the proton transfer is calculated by optimizing the **TS** between a **RC** and a **PC**.

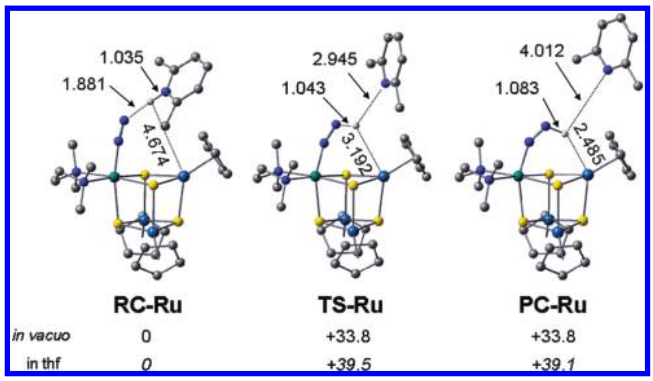

Figure 5. Optimized structures and relative energies of **RC**−**Ru**, **TS**−**Ru**, and **PC**−**Ru** for the proton transfer from $LutH^+$ to $[\mathbf{Ru}(N_2)]$. Interatomic distances are presented in Å. Energies relative to RC−Ru are shown in kcal/mol. Hydrogen atoms except for the transferring proton are omitted for clarity.

Figure 5 shows optimized structures of the **RC**, **TS**, and **PC** for the $[\mathbf{Ru}(N_2)]-LutH^+$ system (denoted by **RC**−**Ru**, **TS**−**Ru**, and **PC**−**Ru**). The reaction of $[\mathbf{Ru}^*(N_2)]$ with $LutH^+$ was not investigated because the optimized structure of $[\mathbf{Ru}^*(N_2H)]^+$ does not have a diazenido group. At the B3LYP/LACV3P+** level of theory, **PC**−**Ru** is calculated to be 33.8 kcal/mol less stable than **RC**−**Ru** and is isoenergetic to **TS**−**Ru**. The proton in **PC**−**Ru** is cooperatively bound by N_2 and Ir1, similar to that of the optimized structure of $[\mathbf{Ru}(N_2H)]^+$. The structure of TS−**Ru** is close to that of **PC**−**Ru**, and trivial structural changes, such as the rotation of the N−H bond around the N−N axis, cause recombination of H^+ and Lut leading to **RC**−**Ru**. Solvation makes the proton transfer more difficult to occur. **PC**−**Ru** in THF is less stable than RC−**Ru** (+39.1 kcal/mol), and the activation barrier for proton transfer becomes higher (+39.5 kcal/mol). These results suggest that the N_2 ligand bound to the $RuIr_3S_4$ core is not protonated with $LutH^+$ at room temperature even if the Cp* ligand on Ir1 is replaced by the Cp ligand.

As described in Figure 6, **RC**−**M** and **PC**−**M** (**M** = Mo and W) are separated by a very low-activation barrier (1.9 kcal/mol for Mo and 0.3 kcal/mol for W in vacuo), and **TS**−**M** has a reasonable imaginary frequency for the N−H bond dissociation (1182*i* for Mo and 1070*i* for W). The activation barriers are estimated to be higher in THF (6.4 kcal/mol for Mo and 1.6 kcal/mol for W). In the proton transfer from $LutH^+$ to $[\mathbf{Mo}(N_2)]$, **RC**−**Mo** and **PC**−**Mo** are nearly isoenergetic; **PC**−**Mo** is 1.7 kcal/mol more stable than **RC**−**Mo** in vacuo and 1.2 kcal/mol less stable than **RC**−**Mo** in THF. It is noteworthy that the protonation of $[\mathbf{W}(N_2)]$ with $LutH^+$ would proceed as a barrierless reaction, and the generated diazenido complex

(29) Sutton, D. *Chem. Rev.* **1993**, *93*, 995.

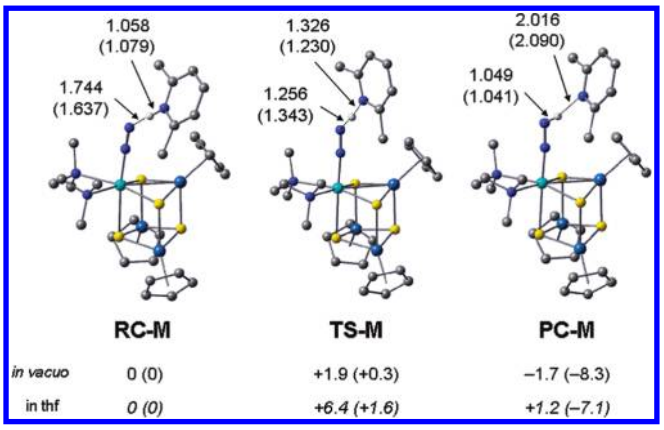

Figure 6. Optimized structures and relative energies of **RC**−**M**, **TS**−**M**, and **PC**−**M** (**M** = Mo and W) for the proton transfer from $LutH^+$ to [**M**(N_2)]. Interatomic distances and relative energies are presented in Å and kcal/mol, respectively. The values calculated for the W core are shown in parentheses. Hydrogen atoms except for the transferring proton are omitted for clarity.

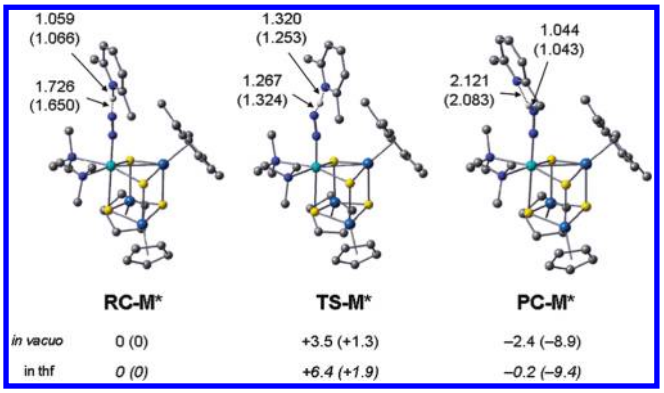

Figure 7. Optimized structures and relative energies of **RC**−**M***, **TS**−**M***, and **PC**−**M*** (**M** = Mo and W) for the proton transfer from $LutH^+$ to [**M***(N_2)]. Interatomic distances and relative energies are presented in Å and kcal/mol, respectively. The values calculated for the W core are shown in parentheses. Hydrogen atoms except for the transferring proton are omitted for clarity.

(**PC**−**W**) is more stable than the dinitrogen complex (**RC**−**W**) by 8.3 kcal/mol in vacuo (7.1 kcal/mol in THF). Figure 7 shows optimized structures of **RC**, **TS**, and **PC** for the [**M***(N_2)]−$LutH^+$ system (**M** = Mo and W). The bulkiness of the ligand on Ir1 does not influence both the structure and energetics of the Mo−N_2 and W−N_2 complexes. **PC**−**Mo*** is slightly more stable than **RC**−**Mo*** even in THF (0.2 kcal/mol), and the activation barrier is calculated to be 3.5 kcal/mol in vacuo and 6.4 kcal/mol in THF, both of which are comparable with the values for the [**Mo**(N_2)]−$LutH^+$ system. **PC**−**W*** is more stable than **RC**−**W*** by 8.9 kcal/mol in vacuo (9.4 kcal/mol in THF), and the activation energy is very small (1.3 kcal/mol in vacuo and 1.9 kcal/mol in THF). These results on the Mo−N_2 and W−N_2 complexes indicate that the Mo and W cores would highly activate the N_2 ligand and that the coordinated N_2 ligand can be directly protonated with $LutH^+$.

It is worthy to note that the Mo(II) and W(II) centers in the $MoIr_3S_4$ and WIr_3S_4 cores can bind N_2 and facilitate the protonation of N_2. The calculated results present a sharp contrast to the previous findings that octahedral Mo and W complexes, which are known to be amenable

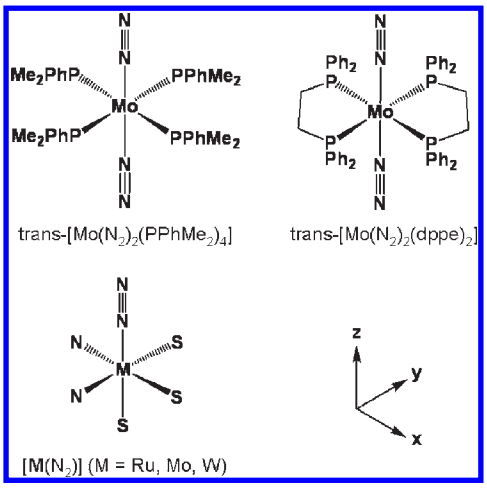

Figure 8. The definition of coordinate axes for the NPA calculation. Only the nearest-neighbor atoms of M are presented for [**M**(N_2)].

to effective protonation at their N_2 ligands, are essentially limited to those containing zerovalent metal centers, e.g., a series of Mo− and W−N_2 complexes with ancillary phosphine ligands.[12] Thus, we would like to compare the electronic structures of [$\mathbf{M^{II}}$(N_2)] (**M** = Ru, Mo, and W) with those of the well-known Mo/W−N_2 complex with phosphine coligands, *trans*-[Mo^0(N_2)$_2$($PPhMe_2$)$_4$] and *trans*-[Mo^0(N_2)$_2$(dppe)$_2$] (dppe = $Ph_2PCH_2CH_2PPh_2$) by using the natural population analysis (NPA). For a simple consideration of interactions among the metal center M, N_2, and ancillary ligands L, we assume that the N_2 ligand interacts with the metal center via σ-donation and π-back-donation, while the ancillary ligands indirectly interact with the N_2 ligand through M. The N_2 ligand gives a certain number of electrons (n_σ) to M via σ-donation (from p_z and s orbitals of N_2 to $d_z{}^2$ and s orbitals of M) and receives a certain number of electrons (n_π) from M via π-back-donation (from d_{xz} and d_{yz} orbitals of M to p_x and p_y orbitals of N_2). The value of $n_\pi - n_\sigma$ roughly corresponds to the total number of excess electrons on N_2. The definition of x, y, and z axes here are presented in Figure 8. The number of electrons donated from L to M (n_L) is calculated with an equation $n_L = (n_M - n_{formal}) + (n_\pi - n_\sigma)$, where n_M is the sum of valence d and s electrons assigned to M, and n_{formal} is the number of valence electrons of M estimated from its formal charge (e.g., n_{formal} of [$\mathbf{Mo^{II}}$(N_2)] is 4). The result of the NPA calculations is summarized in Table 3. In the case of [**Ru**(N_2)], for example, the ancillary ligands donates 1.96 e^- to the central Ru atom. The Ru atom gives 0.37 e^- as a result of a π-back-donation to N_2 and receives 0.30 e^- as a result of a σ-donation from N_2. The NPA charges on Ru and N_2 are +0.11 (8−7.89) and −0.07, respectively. One of the interesting findings is that the cubane framework in [**M**(N_2)] serves as a very strong electron donor to the metal center M, as expected by Mizobe and co-workers.[14] Due to the strong electron-donating ability of the cubane framework, the NPA charge on M is not +2 but close to neutral for all [**M**(N_2)]. Another finding is that the strength of σ-donation (0.30 e^-) is almost similar for all the complexes calculated here. This suggests that the degree of N_2 activation in metal−N_2 complexes is determined by the strength of π-back-donation. Selected

Table 3. Result of the NPA Analysis on the Interaction among the Metal Center M, N_2, and Ancillary Ligands L Calculated for *trans*-$[Mo(N_2)_2(PPhMe_2)_4]$, *trans*-$[Mo^0(N_2)_2(dppe)_2]$ (dppe = $Ph_2PCH_2CH_2PPh_2$), and [**M**(N_2)] (**M** = Ru, Mo, and W)[a]

	$[Mo(N_2)_2(PPhMe_2)_4]$	$[Mo(N_2)_2(dppe)_2]$	[**Ru**(N_2)]	[**Mo**(N_2)]	[**W**(N_2)]
n_σ ($N_2 \rightarrow$ **M**)	0.60[b]	0.62[b]	0.30	0.32	0.33
n_π (**M** $\rightarrow N_2$)	0.88[b]	0.82[b]	0.37	0.62	0.80
$\Delta(n_\pi - n_\sigma)$	0.28[b]	0.20[b]	0.07	0.30	0.47
n_M	7.00	7.06	7.89	5.93	5.72
n_{formal}	6	6	6	4	4
n_L	1.28	1.26	1.96	2.23	2.19

[a] n_σ is the number of σ electrons moved from $N_2 \rightarrow$ M, n_π is the number of π electrons moved from M $\rightarrow N_2$, n_M is the number of valence electrons assigned to M, n_{formal} is the number of valence electrons calculated from the formal charge of M, and n_L is the total number of electrons moved from L $\rightarrow$ M and N_2. [b] The total value of two N_2 ligands.

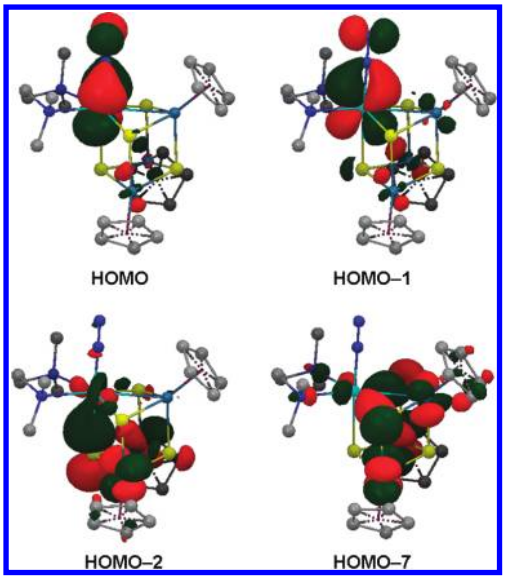

Figure 9. Frontier orbitals of [**Mo**(N_2)] responsible for the Mo−N_2 bonding (HOMO and HOMO−1) and the electron donation from the cubane framework to the Mo center (HOMO−2 and HOMO−7).

frontier orbitals of [**Mo**(N_2)] are depicted in Figure 9 in order to show the π-back-donation from the Mo atom to the N_2 ligand as well as the electron donation from the S atoms consisting of the cubane framework to the Mo atom.

4. Conclusions

In the present study, we have preformed a density functional theory (DFT) study on various cubane-type metal−sulfido clusters ligating dinitrogen, $[(CpIr)_2(RIr)\{M(tmeda)(N_2)\}(\mu_3\text{-}S)_4]$ (M = V, Cr, Mn, Fe, Co, Ni, Cu, Mo, Ru, and W; R = Cp and Cp*), to propose new cubane-type metal−sulfido clusters that can activate dinitrogen more efficiently than the $RuIr_3S_4$ cluster $[(Cp^*Ir)_3\{Ru(tmeda)\}(\mu_3\text{-}S)_4]$ prepared by Mizobe and co-workers.[14] The degree of N_2 activation in the metal−dinitrogen complexes was evaluated based on the three criteria: (i) the N−N bond distance, (ii) N−N vibrational frequency, and (iii) the gross NPA charge on N_2. The gross NPA charge on N_2 would be a good indicator for judging the degree of N_2 activation because the coordinated N_2 must have a negative charge for protonation, which is the first step toward nitrogen fixation. Among the clusters examined here, the $MoIr_3S_4$ and WIr_3S_4 cores exhibit significant N_2-activating ability. These cores bind dinitrogen as strong as the $RuIr_3S_4$ core does, and also the coordinated N_2 to them has a large negative charge on N_2. The bulkiness of the ligand R on Ir1 does not influence the characteristics of N_2 in the M−N_2 complexes (M = Ru, Mo, and W). On the other hand, the protonation of the Cp*-substituted Ru−N_2 complex does not give a corresponding diazenido (−NNH) complex, while the protonation of the Mo−N_2 and W−N_2 complexes results in the formation of diazenido complexes. The reactivity of these three M−N_2 complexes with a proton donor ($LutH^+$) has been discussed from a kinetic aspect by searching a possible reaction pathway of proton transfer. The calculational results on the Ru−N_2 complex imply that the protonation with $LutH^+$ would not occur at room temperature, which is consistent with the present experimental result that Mizobe's Ru−N_2 complex is not protonated at room temperature. For the proton transfer to the Mo−N_2 and W−N_2 complexes, in contrast, high stability of diazenido complexes and small activation energies promise a direct protonation of the N_2 ligand. We conclude from the detailed DFT analysis that the $MoIr_3S_4$ and WIr_3S_4 clusters are best suited for the N_2 activation aiming at functionalization. On the basis of the present result, we have started preparing a new cubane-type metal−sulfido cluster having the $MoIr_3S_4$ and WIr_3S_4 cores. A preliminary result on the newly synthesized $MoIr_3S_4$ cluster has indicated that its formal Mo(II) site can bind CO that is isoelectronic with N_2, whereby the CO ligand exhibits the ν_{CO} band in an extremely low-frequency region, i.e., 1 725 cm^{-1} in $[\{Mo(CO)(dppe)\}(Cp^*Ir)_3(\mu_3\text{-}S)_4]$, in contrast to 1 925 cm^{-1} for $[\{Mo(CO)(dppe)\}(Cp^*Ir)_3(\mu_3\text{-}S)_4]$.[30]

Acknowledgment. K.Y. acknowledges Grants-in-Aid (nos. 18066013 and 18GS0207) for Scientific Research from the Japan Society for the Promotion of Science (JSPS) and the Ministry of Culture, Sports, Science and Technology of Japan (MEXT), the Nanotechnology Support Project of MEXT, and the Joint Project of Chemical Synthesis Core Research Institutions of MEXT for their support of this work.

Supporting Information Available: Atomic Cartesian coordinates for all the structures optimized in the present study. This material is available free of charge via the Internet at http://pubs.acs.org.

(30) Manaka, Y.; Mori, H.; Seino, H.; Mizobe, Y. Presented at the56th Symposium on Organometallic Chemistry,Kyoto,2009 ; Poster P3b-22.